

# Distributionally Consistent Simulation of Naturalistic Driving Environment for Autonomous Vehicle Testing

Xintao Yan<sup>a</sup>, Shuo Feng<sup>a,\*</sup>, Haowei Sun<sup>a</sup>, Henry X. Liu<sup>a,b</sup>

<sup>a</sup>*Department of Civil and Environmental Engineering, University of Michigan, Ann Arbor, MI, USA*

<sup>b</sup>*University of Michigan Transportation Research Institute, University of Michigan, Ann Arbor, MI, USA*

## Abstract

Microscopic traffic simulation provides a controllable, repeatable, and efficient testing environment for autonomous vehicles (AVs). To evaluate AVs' safety performance unbiasedly, ideally, the probability distributions of the joint state space of all vehicles in the simulated naturalistic driving environment (NDE) needs to be consistent with those from the real-world driving environment. However, although human driving behaviors have been extensively investigated in the transportation engineering field, most existing models were developed for traffic flow analysis without consideration of distributional consistency of driving behaviors, which may cause significant evaluation biasedness for AV testing. To fill this research gap, a distributionally consistent NDE modeling framework is proposed. Using large-scale naturalistic driving data, empirical distributions are obtained to construct the stochastic human driving behavior models under different conditions, which serve as the basic behavior models. To reduce the model errors caused by the limited data quantity and mitigate the error accumulation problem during the simulation, an optimization framework is designed to further enhance the basic models. Specifically, the vehicle state evolution is modeled as a Markov chain and its stationary distribution is twisted to match the distribution from the real-world driving environment. In the case study of highway driving environment using real-world naturalistic driving data, the distributional accuracy of the generated NDE is validated. The generated NDE is further utilized to test the safety performance of an AV model to validate its effectiveness.

**Keywords:** Naturalistic driving environment, Driving behavior, Autonomous Vehicle, Testing and evaluation, Simulation

---

\*Corresponding author.

# 1 Introduction

Testing and evaluation is a critical step in the development and deployment of autonomous vehicles (AVs), which has received extensive attention from both the industry and academia in recent years (Kalra and Paddock, 2016; Zhao et al., 2016; Hungar et al., 2017; Koren et al., 2018; O’Kelly et al., 2018; Li et al., 2019a; Feng et al., 2020a,b,c,d; Klischat and Althoff, 2020; Waymo, 2020). Among the three major testing methods (i.e., simulation, test track, and on-road test), simulation provides the most controllable, repeatable, and efficient testing environment (Thorn et al., 2018). To predict AVs’ safety performance in the real world, the prevailing method is to test the AV models in the simulation of the naturalistic driving environment (NDE), observe their performance, and make statistical comparisons to human driver performance (Li et al., 2019b). As the NDE significantly affects the response and performance of AVs, to obtain an accurate prediction of AVs’ performance, the NDE needs to realistically capture human driving behaviors to reproduce a real-world driving environment.

To evaluate an AV’s safety performance, its expected probability of an event of interest (e.g., accident) is usually measured by testing the AV in the NDE (Zhao et al., 2016; Feng et al., 2020a,b). Specifically, if the variables that define the environment are denoted as  $X$ , testing an AV in the real-world driving environment is essential to i.i.d. sample  $X$  from its underlying distribution, denoted as  $X \sim P(X)$ , to estimate its performance  $\mu_E^\kappa$  by

$$\mu_E^\kappa := \mathbb{E}_X (\phi_E^\kappa (X)) \approx \frac{1}{n} \sum_{i=1}^n \phi_E^\kappa (X_i) \approx \frac{m}{n}, X_i \sim P(X), \quad (1)$$

where  $E$  denotes the event of interest,  $\kappa$  denotes the AV agent under test,  $\phi_E^\kappa (X)$  denotes the AV performance at the environment specified by  $X$ ,  $n$  denotes the number of tests, and  $m$  denotes the number of event  $E$  occurred during tests. The last two approximations are derived by Monte Carlo estimation (Owen, 2013). Only with the accurate distribution  $P(X)$  in the simulation, the estimation of  $\mu_E^\kappa$  can be unbiased (i.e., statistically accurate). Therefore, to evaluate the AV performance accurately, the NDE model needs to be distributionally consistent with the real-world driving environment, which is a challenging requirement.

Although the NDE modeling has been studied extensively in the transportation engineering field, few existing NDE models serve the purpose for AV testing. A general form of the existing driving behavior model can be expressed by

$$u(t) = \psi(Y(t), \theta(t)) + \epsilon(t), \quad (2)$$

where  $t$  denotes the time,  $u(t)$  denotes the action (e.g., longitudinal and lateral acceleration) of the vehicle at the  $t$ -th time instance,  $Y(t)$  denotes the states of the ego-vehicle and surrounding vehicles that have an influence on the ego-vehicle decision making,  $\psi(\cdot)$  denotes a parametric model that maps from the state space to the action space,  $\theta(t)$  denotes model parameters that could be deterministic or stochastic, and  $\epsilon(t)$  denotes the external noise term of the behavior model which follows a certain distribution. Most existing models are deterministic and cannot capture the stochastic nature of human driving behaviors. For these models, the model parameters  $\theta$  remain fixed during the simulation and no external noise term  $\epsilon$  is added. For example, most well-known conventional behavior models fall into this category, such as the Wiedemann model (Wiedemann, 1974), the Gipps model (Gipps, 1981), and the intelligent driver model (IDM) (Treiber et al., 2000) for car-following behaviors as well as the Gipps lane-changing model (Gipps, 1986) and the Minimizing Overall Braking Induced by Lane Changes (MOBIL) model (Kesting et al., 2007) for

lane-changing behaviors. Although the parameters of these models can be calibrated using real-world data (Punzo et al., 2012; Sangster et al., 2013; Li et al., 2016; Zhu et al., 2018a; Osorio and Punzo, 2019), they cannot capture the stochastic behaviors of human drivers. Recently, increasing studies have used advanced machine learning-based methods to fit the behavior model  $\psi$  using a neural network. By utilizing large-scale naturalistic driving datasets, these methods aim to better reproduce the observed trajectories of human drivers. For example, the deep neural network is widely applied, such as the recurrent neural network (RNN) and long short-term memory (LSTM) neural network (Wang et al., 2017; Huang et al., 2018; Zhang et al., 2019; Xie et al., 2019). Zhu et al. (2018b) used deep reinforcement learning (DRL) to learn human-like car-following behavior from trial and error. However, the same problem of lacking stochasticity still exists for these methods.

The stochasticity can be incorporated into the model by introducing external noise term  $\epsilon(t)$  and/or stochasticity to model parameters  $\theta(t)$ . However, most existing models were designed for the traffic flow analysis purpose, such as to reproduce the representative traffic characteristics (e.g., traffic oscillations and the fundamental diagram) observed in the real world. Consequently, these models usually do not pay much attention to the distributional accuracy of stochastic driving behaviors. This inaccuracy may not affect significantly for the traffic flow analysis, but will cause significant evaluation biasedness on AV performance. To incorporate the external noise term  $\epsilon(t)$ , the most commonly used one is the Gaussian noise (Laval et al., 2014; He et al., 2015; Treiber and Kesting, 2017; Kuefler et al., 2017; Bhattacharyya et al., 2020). For example, Laval et al. (2014) added an external Gaussian noise to Newell’s car-following model (Newell, 2002) and showed that the stochastic car-following model can produce traffic oscillations that accord well with the observations. He et al. (2015) exhibited a similar result that stop-and-go oscillations can be reproduced by adding a Gaussian noise to a deterministic data-driven car-following model based on the k-nearest neighbor. Kuefler et al. (2017) and Bhattacharyya et al. (2020) applied Generative Adversarial Imitation Learning (GAIL) to model human driving behaviors on the highway where the output action follows a Gaussian distribution. However, the external addition of the Gaussian noise cannot realistically and accurately depict human stochastic driving behaviors. Many researchers have shown the asymmetric driving behavior of human drivers so the stochasticity is generally not symmetric as Gaussian (Newell, 1965; Yeo, 2008; Yang and Peng, 2010; Li and Chen, 2017). Moreover, as pointed out in Jabari et al. (2014), directly introducing Gaussian randomness would potentially allow for physically unrealistic quantities (e.g., negative speeds). To account for the asymmetric property, the extreme value distribution noise is applied in Yang and Peng (2010) to generate a stochastic car-following model. Although this distribution is more realistic than the Gaussian noise, it still suffers from limited accuracy due to the limited model flexibility for fitting complicated driving behaviors, especially for safety-critical situations.

Besides adding an external noise  $\epsilon(t)$ , the stochasticity can also be incorporated in model parameters  $\theta(t)$ . However, existing models do not concern with the distributional accuracy of the driving behaviors after the stochasticity is introduced. To investigate the different traffic oscillation generation mechanisms, Treiber and Kesting (2017) proposed a general form for stochastic car-following models, where both the external noise (Gaussian noise) and stochastic model parameters are considered. The indifference regions in the form of action points are included in the model, so the new acceleration will be executed only when the change is greater than a threshold parameter, which follows a uniform distribution. The human error-inducing behaviors are considered in Yang and Peng (2010) including perceptual limitation, time delay, and distraction. The length of the time delay and the distraction interval were fitted by exponential distribution and lognormal distribution according to real-world data, respectively. These effects were incorporated as influencing parameters and sampled at each decision moment, which leads to a stochastic car-following model. Hamdar et al. (2008, 2015) proposed a utility-based stochastic car-following model where accelera-

tion probability follows a continuous logit model. The utility of a specific acceleration under a given state is composed of the prospect-theoretic acceleration utility derived by the prospect theory and the penalty utility for the risk of the rear-end collision. To calculate the penalty utility value, the estimated leading vehicle speed is assumed to follow a Gaussian distribution within the prediction horizon, and therefore, with this stochastic parameter, the penalty utility also follows a Gaussian distribution and results in a stochastic model. However, although the simulated fundamental diagram was examined, whether the acceleration distribution is accurate was not considered.

Notwithstanding the related studies, most existing methods are either deterministic or adding simple stochasticity for traffic flow analysis purposes, which cannot capture the accurate distribution of stochastic human driving behaviors. Therefore, the driving environment that is generated by these behavior models cannot accurately reproduce the stochastic properties of the NDE, which is critical for AV testing. There was one notable exception that in [Chen et al. \(2010\)](#), the authors proposed a stochastic car-following model to capture the distribution of time headway. Moreover, it is challenging to generate a distributionally accurate NDE using stochastic behavior models, because of the high dimensionality of the driving environment, which is caused by the complex interactions among a large number of vehicles for a long horizon. Consequently, a small inaccuracy of vehicle behavior distribution will be accumulated and compounded during the simulation, which would cause significant deviation from the realistic environment. This error accumulation issue, which has not been considered by existing studies (even in [Chen et al. \(2010\)](#)), is critically important when constructing the NDE for AV testing purposes.

In this paper, to solve the abovementioned issues, we propose a distributionally consistent NDE modeling framework for AV testing purposes, considering both longitudinal and lateral behaviors of vehicles. To simplify the problem, both the temporal and spatial structures of the environment will be exploited. For the temporal structure, Markovian properties will be applied, which indicates that the action of the next timestep only depends on the current state. For the spatial structure, domain knowledge will be introduced to relax the spatial dependencies between ego-vehicle action and other vehicle states. To accurately capture the stochastic behaviors and maintain the microscopic fidelity, we first propose to directly estimate behavior models using empirical distributions from the large-scale naturalistic driving data (NDD). These empirical behavior models serve as basic models. If the dataset is sufficiently accurate, diverse, and large, the empirical distributions can well characterize human driving behaviors in different situations. However, as the limitation of data quantity and inevitable data noise, the obtained empirical distributions may also be inaccurate. As discussed previously, the inaccuracy can be accumulated and compounded with the simulation, then the resultant simulation environment will significantly deviate from the realistic environment. To address this issue, we further design an optimization mechanism, which can reduce the accumulated errors by adjustments of the basic models. Specifically, the vehicle state evolution is modeled as a Markov chain, and its stationary distribution is twisted to match the real-world driving environment, by optimizing the empirical longitudinal acceleration distributions. Instead of considering all features of the environment, a subset of the environment feature that is critical for the AV testing (e.g., speed and spacing) is chosen, and only the stationary distribution of this feature is optimized. Therefore, the generated NDE is guaranteed to distributionally match the real-world driving environment in terms of the critical feature throughout the simulation, which is a necessary condition for a required NDE model. Using the large-scale real-world NDD collected by the University of Michigan, Ann Arbor, we validate the performance of the proposed method for a multilane highway driving environment. Comparing with existing models, the proposed method demonstrates superior performance. To further validate the capability for AV testing, the generated NDE is utilized to test the safety performance of an AV model. The experiments show that the generated NDE can effectively evaluate AV safety performance and produce diverse accident cases

that are valuable for AV development.

The main contributions of this paper are fourfold: (1) we identify the research gap that new NDE modeling techniques are critically needed since existing methods cannot achieve sufficient stochastic behavior accuracy and therefore cannot be applied directly for AV testing purposes; (2) a data-driven method is proposed for generating the empirical behavior models which can serve as the basic behavior models; (3) a robust modeling framework is proposed to optimize the empirical behavior models and generate the NDE that is distributionally consistent with the real-world driving environment during the simulation; (4) the proposed method is validated using real-world NDD and the generated NDE is further validated for testing an AV model.

The rest of this paper is organized as follows. In section 2, we first introduce the empirical NDE modeling method including the data-driven initialization method and empirical behavior models. In section 3, to account for the error accumulation problem and obtain a distributionally consistent NDE, the robust modeling framework is proposed to further optimize the empirical behavior models. In section 4, using real-world NDD, we validate the performance of the proposed method and compare it with existing models for a multilane highway driving environment. An AV testing experiment is further conducted using the proposed NDE in this section. Finally, section 5 concludes the paper and lays out some future directions.

## 2 Empirical NDE modeling method

This section introduces the empirical NDE modeling method based on the empirical distributions from NDD, including the data-driven initialization method and empirical behavior models. In section 2.1, to make the NDE modeling tractable, we model the environment as a Markov chain and assume spatiotemporal independency, which is commonly used in the transportation domain. Then, the data-driven initialization method is proposed in section 2.2, and the empirical behavior model is introduced and discussed in section 2.3.

### 2.1 NDE modeling

In this study, the NDE is represented by two categories of variables. The first one is predetermined by the operational design domain (United States. Department of Transportation, 2020; Waymo, 2020), such as weather condition, traffic rules, etc., which remains static throughout the simulation. The second one is stochastic and may vary in each simulation instantiation, such as initial states of vehicles, actions of vehicles during the simulation, etc. The latter one is what the NDE modeling concerns and can be represented as

$$X = [ S_0 \quad \cdots \quad S_T ] = \begin{bmatrix} s_0^1 & \cdots & s_T^1 \\ \vdots & \ddots & \vdots \\ s_0^N & \cdots & s_T^N \end{bmatrix}, X \in \mathcal{X}, \quad (3)$$

where  $X$  denotes an instantiation of the NDE,  $\mathcal{X}$  denotes the feasible space (all possible driving situations) of NDE,  $s_t^i$  denotes the states (e.g., position and speed) of the  $i$ -th vehicle (more generally, road user) at the  $t$ -th time step,  $S_t = [ s_t^1 \quad \cdots \quad s_t^N ]^\top \in \mathcal{S}$  denotes the state of the NDE at the  $t$ -th time step,  $\mathcal{S}$  denotes the state space,  $N$  denotes the number of vehicles in the simulation, and  $T$  denotes the total number of time steps. As indicated in Eq. (3), the NDE could be extremely high dimensional due to a large number of vehicles and a long simulation horizon. To make the  $P(X)$  tractable, in this study, the NDE is modeled as a Markov chain, and spatiotemporal independency

assumptions will be applied to simplify the modeling process. Also, we consider the discretized and bounded position and velocity so the state space is finite.

For AV testing, an objective and quantitative safety performance measurement is the AV accident rate, which has been widely applied (Kalra and Paddock, 2016; Zhao et al., 2016; Feng et al., 2020a,b). Therefore, to calculate the expected accident rate  $\mu_E^\kappa := \mathbb{E}_X(\phi_E^\kappa(X))$ , we need to know the probability density function of the AV performance  $\phi_E^\kappa(X)$  under all driving environment  $X$ , which is clearly not achievable. To address this issue, the Monte Carlo method is usually applied to approximate the accident rate. This is essentially the idea of the on-road test, which deploys the AV in the real world, lets it interact with the realistic traffic, and observes its performance (i.e., an accident happens or not). As pointed out in Kalra and Paddock (2016), however, in order to obtain an accurate estimation result, it would take tens and even hundreds of years to drive the desired miles using the on-road test. Therefore, the simulation test becomes a promising alternative. To obtain an unbiased evaluation, ideally, the probability distributions of the joint state space of all vehicles in the simulated NDE needs to be consistent with those from the real-world driving environment, which is denoted as  $X \sim P(X)$ .

The generation method of the NDE includes two main components. The first one is the initialization method which determines the environment initial state  $S_0$ , and the second one is vehicle behavior models, i.e., how vehicles interact with each other, which governs future states of the environment after the initial state. Given an initial state, the evolution of the environment can be modeled as a Markov chain as shown in 1, where  $U_t = [u_t^1 \ \cdots \ u_t^N]^\top$  denotes maneuvers of all vehicles at the  $t$ -th time step and  $u_t^i$  denotes the maneuver (longitudinal and lateral accelerations) of the  $i$ -th vehicle at the moment. In this paper, we consider discretized and bounded maneuvers of vehicles. Two commonly used assumptions are adopted here. The first one is the Markovian property that vehicle action at the current timestep only depends on the environment state at the current step. Another assumption is that all vehicles share a common and constant sensing-action cycle, which is commonly accepted in the robotics motion planning region (Bareiss and van den Berg, 2015), therefore, all vehicles choose their actions simultaneously and maintain these actions until the next decision moment. Therefore, the probability of the NDE can be written in a factorized way as

$$P(X) = P(S_0) \times \prod_{t=0}^{T-1} P(S_{t+1}|S_t), \quad (4)$$

where  $P(S_0)$  denotes the initial state probability, and  $P(S_{t+1}|S_t)$  denotes the state transition probability which can be expressed as

$$P(S_{t+1}|S_t) = P(U_t|S_t). \quad (5)$$

To simplify the problem, we also assume that all vehicles choose their maneuvers independently so we have

$$P(U_t|S_t) = \prod_{i=1}^N P(u_t^i|S_t). \quad (6)$$

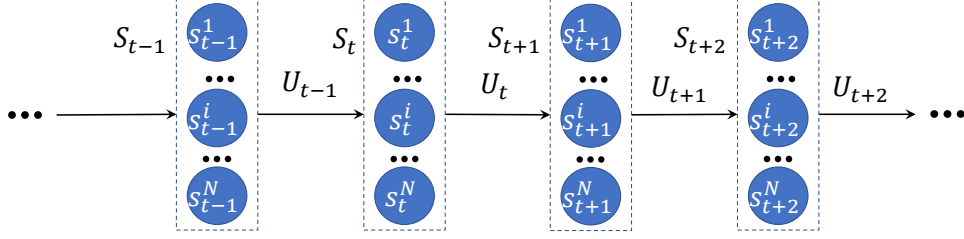


Figure 1: The Markov chain of the NDE

To further simplify  $P(u_t^i|S_t)$  in Eq. (6), domain knowledge will be introduced later to relax the spatial dependency such that the vehicle action will solely concern with its surrounding vehicles rather than all vehicles on the road. Let  $Z_t^i \subseteq S_t$  be the states of all vehicles that have influences with the  $i$ -th vehicle's maneuver decision at  $t$ -th moment. Therefore, the maneuver probability of the  $i$ -th vehicle at  $t$ -th time step can be rewritten as

$$P(u_t^i|S_t) = P(u_t^i|Z_t^i). \quad (7)$$

Finally, the probability of the NDE can be derived as

$$P(X) = P(S_0) \times \prod_{t=0}^{T-1} \prod_{i=1}^N P(u_t^i|Z_t^i). \quad (8)$$

Therefore, based on the initialization, the NDE can be generated by simulations according to the maneuver probability  $P(u_t^i|Z_t^i)$ .

Let  $\mathcal{Z}$  be the space of vehicles states that determine the vehicle maneuver distribution. Then  $\forall Z \in \mathcal{Z}, \exists S \in \mathcal{S}$ , such that  $Z \subseteq S$ . Note that the size of  $\mathcal{Z}$  is significantly smaller than  $\mathcal{S}$  since only surrounding vehicles will influence the decision making. In this study, the vehicle maneuvers are discretized into two types: left/right lane change, and longitudinal accelerations. The action space is denoted as  $\mathcal{A}$ . Therefore, the vehicle behavior model  $F \in \mathbb{R}^{|\mathcal{Z}| \times |\mathcal{A}|}$  can be represented as

$$F = [ f(Z^1) \quad \dots \quad f(Z^{|\mathcal{Z}|}) ], \quad (9)$$

where  $|\mathcal{A}|$  and  $|\mathcal{Z}|$  are the size of vehicle action space and vehicle action-dependent state space, respectively, and  $f(Z) := [ \dots P(u|Z) \dots ]^T \in \mathbb{R}^{|\mathcal{A}| \times 1}, \forall Z \in \mathcal{Z}$  is the maneuver probability mass function of a vehicle given its surrounding vehicles information. Therefore, the goal of NDE modeling is essentially to model the stochastic behavior models  $F \in \mathbb{R}^{|\mathcal{Z}| \times |\mathcal{A}|}$  for all the action space and action-dependent state space.

## 2.2 Data-driven initialization method

The simulation initialization method determines the initial state of all vehicles, which include the position and speed, etc. A realistic initialization is preferred to shorten the required warm-up time, which can improve the simulation efficiency. We propose a data-driven initialization method to sequentially determine the state  $s_0^i = [pos_0^i(x), pos_0^i(y), v_0^i]$ , i.e., longitudinal position, lateral position, and velocity, of downstream vehicles based on the upstream vehicles states. The lateral

position  $pos_0^i(y)$  is the same as the lateral coordinates of its lane center. The first vehicle of each lane is determined by sampling its longitudinal position inside an initial zone from a uniform distribution and its velocity from the empirical velocity distribution. This can be expressed as

$$pos_0^1(x) \sim U(0, d_0), \quad (10)$$

$$v_0^1 \sim \pi_v^*, \quad (11)$$

where  $d_0$  is a predetermined initial zone size,  $v_0^1$  is the speed, and  $\pi_v^*$  is the empirical velocity distribution obtained from the NDD. Then an indicator variable follows a Bernoulli distribution  $I_i \sim B(p_{CF})$  is sampled to determine whether this vehicle is in the car-following ( $I_i = 1$ ) situation or free-driving ( $I_i = 0$ ) situation.  $p_{CF}$  is the probability a vehicle is in the car-following case, which can be approximated from NDD. Then the joint distribution of range (spacing)  $r$  and range rate (relative speed)  $rr$  given the current speed  $g(r, rr|v_0^i)$  is queried from the NDD if  $I_i = 1$ . Then, the position and velocity of the next (downstream) vehicle can be obtained by

$$pos_0^{i+1}(x) = pos_0^i(x) + r, \quad (12)$$

$$pos_0^{i+1}(y) = pos_0^i(y), \quad (13)$$

$$v_0^{i+1} = v_0^i + rr, \quad (14)$$

where  $r, rr$  is the range and range rate sampled from  $g(r, rr|v_0^i)$ , and the lateral position of the  $(i + 1)$ -th vehicle is the same as the  $i$ -th vehicle. If  $I_i = 0$ , the next vehicle is randomly generated in a new initial zone outside the car-following observation range, and the velocity follows the empirical velocity distribution. It can be represented as

$$pos_0^{i+1}(x) = pos_0^i(x) + d_{obs} + r, \quad (15)$$

$$r \sim U(0, d_0), \quad (16)$$

$$pos_0^{i+1}(y) = pos_0^i(y), \quad (17)$$

$$v_0^{i+1} \sim \pi_v^*, \quad (18)$$

where  $d_{obs}$  is the predetermined car-following observation range suggested by the NDD. Vehicles on each lane can be sequentially generated by repeating this process.

### 2.3 Empirical behavior models

As the behaviors of background vehicles significantly affect the AV performance, the behavior models are critical for the NDE modeling, which is the focus of this paper. Only with naturalistic probabilistic distributions of behaviors, simulation results can predict the performance of the AV in the real world unbiasedly. The most straightforward way is to directly estimate the empirical behavior models from NDD. The NDD records the human driving behaviors and ego vehicle's surrounding information, for example, the leading vehicle speed and position, etc., in the real-world driving environment. Using the NDD, we can obtain the empirical probability  $P(u|Z), \forall u \in \mathcal{A}, Z \in \mathcal{Z}$  of vehicle maneuvers in different states, which is the empirical approximation of the behavior model  $F$  in Eq. (9), denoted as  $F^*$ .

Note that the empirical behavior models are the histogram density estimators of the real-world human driving behaviors. They are consistent estimators, i.e., converge in probability, to the real behavior models, if the following requirements are satisfied: (1) the data is i.i.d. collected from



the real-world driving behavior models, (2) the data size is sufficiently large, and (3) the action resolution is infinitely high (Shalizi, 2016). The detailed proof can be found in the Appendix. A. Although these requirements are too ideal for practical applications, the empirical behavior models are a good foundation for the NDE modeling, especially considering the fact that larger-scale and higher-quality NDD can be obtained with the deployment of vehicle-based perception sensors.

However, as the limitation of data quantity and data noises are inevitable, and violations of the i.i.d. assumption, the obtained empirical models usually have errors in distribution. As the NDE involves complex interactions among multiple vehicles for a long horizon, the errors of behavior models would accumulate and compound during the simulation, which makes the resultant environment significantly different from the real-world driving situation. Illustration of the error accumulation problem will be provided in the case study in section 4.3 with real-world NDD. To address this issue, the robust modeling framework will be introduced in the next section to further enhance the empirical models.

### 3 Robust modeling framework

The goal of the robust modeling framework is to further adjust the empirical behavior models to address the error accumulation issue discussed above. Because of the limitation of data quantity and quality, the ground truth of the NDE underlying probability distribution is unknown from the data analysis, so the error accumulation cannot be measured directly. To overcome this issue, we propose to match marginal distributions of specific features (speed and spacing) of the NDE which are important for AV testing. Because these features are much lower-dimensional than the environment, their distributions can be approximated from the NDD and serve as the ground truth. As the environment is modeled as a Markov process, the simulated feature distribution can be analytically calculated from the stationary distribution of the Markov process. Therefore, the accumulated error can be measured by comparing the stationary feature distribution and its ground truth. The detailed process of the accumulated error measurement is discussed in section 3.1. By minimizing the accumulated error, the empirical behavior models can be improved toward to result in an accurate real-world driving environment for the AV testing purpose. The proposed optimization method is given in section 3.2. To efficiently solve the optimization problem, in this study, we apply the proposed method to optimize the empirical longitudinal behavior models as a proof of concept, while keeping the empirical lateral behavior models unchanged, which is elaborated in section 3.3.

#### 3.1 Measurement of the accumulated error

In order to solve the error accumulation problem, we first need to measure the accumulated error of the NDE generated by the empirical behavior models. One possible way is to simulate the NDE, collect the data, and obtain the simulated NDE distribution. However, the computational burden of this method is very heavy since a large number of simulations are needed to obtain an accurate estimation, and, especially that, each simulation needs to run a long time horizon to fully observe the error accumulation process. To overcome this problem, we propose to measure the NDE distribution by analyzing the stationary distribution of the NDE Markov chain. By using this analytical method, the NDE stationary distribution serves as an accurate approximation of the simulated environment and reflects the performance of the empirical behavior models. If we have the ground truth of the real-world driving environment, then we can measure the accumulated error by comparing it with the NDE stationary distribution.

We will first show that a stationary distribution exists for the NDE Markov chain under a mild assumption. Based on the section 2.1, the evolution of the NDE is modeled as a time-homogeneous finite Markov chain. We assume it is irreducible which means all states communicate with each other, i.e., a driving situation can lead to any other situation. Then this finite irreducible Markov chain is also aperiodic since there are self-transitions in the chain, which means there exists a state such that the probability of the state at the next time step is the same as the current state is greater than zero. For example, consider all vehicles have the same speed and the state remains the same when all vehicles choose acceleration equals zero. Since the NDE Markov chain is finite, irreducible, and aperiodic, there exists a unique positive stationary distribution (Grimmett and Stirzaker, 2020)  $\pi \in \mathbb{R}^{|\mathcal{S}| \times 1}$  satisfying

$$\pi \succcurlyeq 0, \tag{19}$$

$$\sum_{S \in \mathcal{S}} \pi_S = 1, \tag{20}$$

$$\pi^T \mathbf{P} = \pi^T, \tag{21}$$

where  $\mathbf{P}$  is the state transition probability matrix of the NDE Markov chain.

After the stationary distribution  $\pi$  is obtained, the next step is to obtain the ground truth distribution of the real-world driving environment. However, the dimension of the distribution is extremely high since the joint state space of all vehicles  $\mathcal{S}$  is extremely large. Therefore, the ground truth of the real-world driving environment is usually unknown due to the data limitation. To tackle this challenge, we propose to choose a feature set  $M$  of the environment and approximate the ground truth of these features distribution  $\pi_m^*, m \in M$ , from NDD. Comparing with empirical behavior models, since the environment feature (e.g., vehicle speed) is low dimensional, its empirical distribution from the data is more reliable and robust to data noise and thus can be considered as the ground truth. For AV testing purposes, the speed and spacing between vehicles are two important environment features. Then  $\pi_m^*, m \in M$  include the empirical speed and spacing distribution obtained from the NDD, which can be considered as the ground truth and needed to be matched. Consequently, the key idea is to match the stationary feature distribution with its empirical ground truth, rather than match the entire stationary distribution of the joint state space. Although it is a necessary yet insufficient condition for reproducing a distributionally consistent NDE, as the selected features are critical for the AV testing, matching the feature distribution can much improve the resulting environment.

Mathematically, matching the stationary feature distribution with its empirical ground truth can be expressed as

$$H_m(\pi) = \pi_m^*, \forall m \in M, \tag{22}$$

where  $M$  denotes the selected feature set,  $\pi_m^*$  denotes the empirical distribution of the  $m$ -th feature derived from the NDD, and  $H_m(\cdot)$  is the linear transformation from the Markov chain stationary distribution of all dimensions to the  $m$ -th feature distribution, which aggregates all other dimensions except for the concerned one. For example, the Markov chain stationary distribution depicts the probability distribution of all vehicles position and speed, and then  $H_m(\cdot)$  marginalize it to get the speed distribution of all vehicles.

### 3.2 Optimization of empirical behavior models

After measuring the accumulated error generated by empirical behavior models, the optimization formulation of empirical behavior models will be elaborated in this section, including other con-

straints as discussed below. The vehicle state can be updated based on current state and action as

$$v_{t+1}^i(x) = v_t^i(x) + a_t^i(x) \cdot \Delta t, \quad (23)$$

$$pos_{t+1}^i(x) = pos_t^i(x) + v_t^i(x) \cdot \Delta t + \frac{1}{2} \cdot a_t^i(x) \cdot (\Delta t)^2, \quad (24)$$

where  $pos_t^i(x), v_t^i(x)$  are the positions and speeds on the longitudinal axis of the  $i$ -th vehicle at the current time step  $t$ , respectively. And  $pos_{t+1}^i(x), v_{t+1}^i(x)$  are corresponding values at the next time step  $t + 1$ .  $a_t^i(x)$  is the vehicle longitudinal acceleration, and  $\Delta t$  is the time interval between two decision moments. Similarly, the lateral position and speed can be updated using the lateral acceleration. Therefore, considering the state propagation of all vehicles, the state transition matrix of the Markov chain can be represented in terms of the behavior model as

$$G(F) = \mathbf{P}(S_t, S_{t+1}), \forall S_t, S_{t+1} \in \mathcal{S}, \quad (25)$$

where  $\mathbf{P}(S_t, S_{t+1})$  denotes the transition probability from state  $S_t$  to  $S_{t+1}$ , and  $G(\cdot)$  is a mapping from the behavior model to the transition probability.

Since  $\forall Z \in \mathcal{Z}$ ,  $f(Z)$  is the maneuver probability mass function, the behavior model needs to satisfy the following

$$\sum_{u \in \mathcal{A}} f(u|Z) = 1, \forall Z \in \mathcal{Z}, \quad (26)$$

$$F \succcurlyeq 0, \quad (27)$$

where the summation of all maneuvers probability for any given state equals 1, and any maneuver probability is greater than or equals to zero. Similarly, the state transition matrix has the following properties

$$\sum_{S_{t+1} \in \mathcal{S}} \mathbf{P}(S_t, S_{t+1}) = 1, \forall S_t \in \mathcal{S}, \quad (28)$$

$$\mathbf{P} \succcurlyeq 0, \quad (29)$$

where the summation of each row in the state transition probability matrix equals one and any state transition probability is greater than or equals to zero.

The goal of the optimization is to adjust the empirical behavior models to satisfy the distributional consistency of the environment feature. It is noticed that there may be multiple solutions that achieve the same purpose. Therefore, the objective is to minimize the adjustment to the empirical behavior model. Noting that NDD is the major information source of the NDE modeling, the optimization method will help adjust the data-driven empirical behavior models carefully to prevent introducing new errors. The Frobenius norm is adopted to measure the distance. As a result, combining all constraints, the general formulation of the optimization problem is summarized below

$$\text{minimize} \quad \|F - F^*\|_{Frob} \quad (30)$$

$$\text{subject to} \quad \pi^T \mathbf{P} = \pi^T, \quad (31)$$

$$H_m(\pi) = \pi_m^*, \forall m \in M, \quad (32)$$

$$G(F) = \mathbf{P}(S_t, S_{t+1}), \forall S_t, S_{t+1} \in \mathcal{S}, \quad (33)$$

$$\sum_{u \in \mathcal{A}} f(u|Z) = 1, \forall Z \in \mathcal{Z}, \quad (34)$$

$$\sum_{S_{t+1} \in \mathcal{S}} \mathbf{P}(S_t, S_{t+1}) = 1, \forall S_t \in \mathcal{S}, \quad (35)$$

$$\sum_{S \in \mathcal{S}} \pi_S = 1, \quad (36)$$

$$F, \mathbf{P}, \pi \succeq 0, \quad (37)$$

where optimization variables include the optimized behavior model  $F$ , the state transition probability matrix  $\mathbf{P}$ , and the stationary distribution  $\pi$  of the Markov chain. Note again that  $F^*$  and  $\pi_m^*$  are empirical behavior models and empirical environment feature distribution obtained from the NDD.

### 3.3 Longitudinal behavior model optimization

Although the proposed optimization method is theoretically generic, to simplify the computational complexity, in this study, we apply the proposed method to optimize the empirical longitudinal behavior models as a proof of concept, while keeping the empirical lateral maneuver models unchanged. As the longitudinal behavior models include two scenarios, i.e., free-driving and car-following, two different Markov chains will be constructed and considered, separately. In this paper, for model simplicity, we choose speed as the environment feature in the optimization problem constraint. Then, we examine the simulated speed and spacing distributions and validate their distributional consistency.

For the free-driving case, vehicle longitudinal acceleration depends only on its current speed. In this case, the Markov chain of the NDE degenerates to the speed transition of each vehicle along the time for two reasons. The first one is that the maneuver of each vehicle only depends on its own state, so the original Markov chain can be decomposed into individual Markov chains of each vehicle. The second one is that since the speed is the environment feature that in the constraints, we can consider the speed transition and aggregate the position dimension for a compact representation. Therefore, the transformation  $H(\cdot)$  in constraint (32) becomes a self-mapping, and the decision variable  $\pi$  becomes a known vector and decoupled with  $\mathbf{P}$  in constraint (31). As a result, constraints (31) and (32) can be combined together to a single set of linear constraints as

$$(\pi^*)^T \mathbf{P} = (\pi^*)^T. \quad (38)$$

Note that the mapping function  $G(\cdot)$  in constraint (33) is also a linear mapping here, which finds longitudinal accelerations from the free-driving behavior model to transit the speed from the current moment to the next. Then the formulation for this case becomes a convex optimization problem, which is computationally efficient to solve.

For the car-following case, however, the formulation is not convex. The main reason is that the state of the Markov chain cannot be directly decomposed as the free-driving case, since each vehicle's state transition depends on its leading vehicle. As a result, decision variables are coupled

together in constraint (31), and the mapping function  $G(\cdot)$  in constraint (33) is not linear. To tackle these problems and obtain a tractable solution, two relaxations are applied on the state space of the Markov chain for mathematical simplification. The first one is that we consider the single-vehicle state evolution, and the second one is that the state of the Markov chain is chosen the same as the environment feature. This can be viewed as an aggregated Markov chain where only the dimension of the concerned is retained and all other dimensions are marginalized. By doing so, we generate a simpler model but still with good approximation accuracy. Therefore, the stationary distribution also becomes a known vector from the NDD and decoupled with the transition matrix. The mapping function  $G(\cdot)$  now is also a linear mapping, where the difference with the free-driving case is that an aggregation process is included to marginalize dimensions of the behavior model, for example, the range (spacing) and range rate (relative speed). Then, the car-following case also becomes a convex optimization problem and therefore can be solved efficiently by existing solvers.

## 4 Case study: Highway driving environment

In the case study, we implement the proposed method to generate a multilane highway NDE, which is an important environment for the AV testing. The performance of existing methods is demonstrated to compare with the proposed method. To further validate the capability of the proposed NDE for AV testing purposes, an AV testing experiment is conducted using the generated NDE.

### 4.1 Empirical behavior models

We first introduce how to model vehicle behavior models  $F$  in different situations. The longitudinal and lateral behavior of a vehicle is decomposed into six categories as shown in Figure 2, where the maneuver dependencies with surrounding vehicles are indicated. Specifically, the longitudinal action is categorized into free-driving and car-following scenarios. The acceleration only depends on the velocity of the ego-vehicle in the former case and depends on velocity, range (spacing), and range rate (relative speed) of the ego-vehicle and the preceding vehicle in the later case. The ego-vehicle is considered in the free-driving scenario when there is no vehicle in front of it, where the distance threshold is set as 115 meters as indicated by the NDD. Similarly, the lane-changing scenarios are categorized into four different cases in terms of the different surrounding situations. At each decision moment, a vehicle has 33 possible maneuvers: left lane change, 31 longitudinal accelerations (range from  $-4$  to  $2 \text{ m/s}^2$  with  $0.2$  as the discrete resolution), right lane change. To simplify the maneuver, longitudinal acceleration is assumed zero if the lane-changing decision is made at this moment.

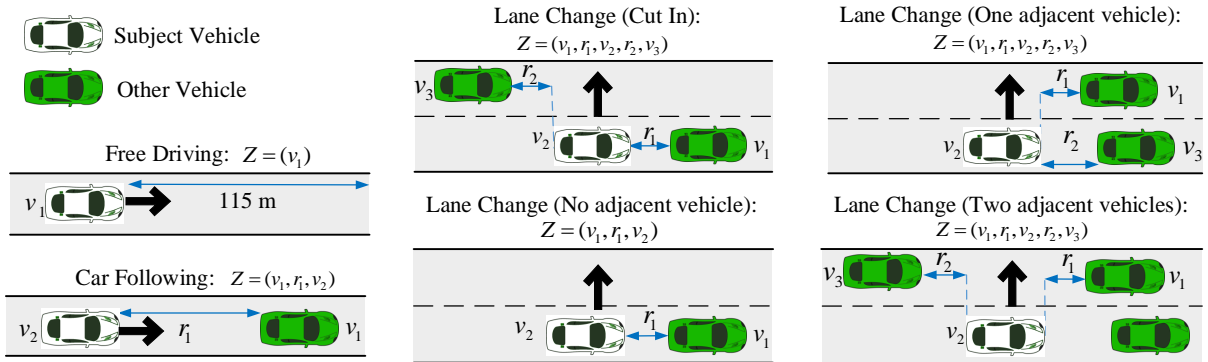


Figure 2: Longitudinal and lateral action categorization.

We utilized the NDD from the Integrated Vehicle Based Safety System (IVBSS) dataset (Sayer et al., 2011) and the Safety Pilot Model Deployment (SPMD) dataset (Bezzina and Sayer, 2014) at the University of Michigan Transportation Research Institute (UMTRI). In the IVBSS program, 108 drivers range from 20 to 70 years old were recruited. Each participant drove the IVBSS vehicle equipped with the data acquisition system (DAS) for 6 weeks. The relative distance and speed with the leading vehicle are recorded by radar in 10 Hz. The SPMD program covered over 34.9 million travel miles and included 98 vehicles equipped with the DAS and Mobileye to record human naturalistic driving behaviors. The data were also recorded at 10 Hz with positions, speeds, and accelerations of ego-vehicles, relative speeds with surrounding vehicles, and both longitudinal and lateral distances between vehicles and lane markings. We queried partial datasets with the following criteria: (1) vehicle was traveling at a speed between 20  $m/s$  and 40  $m/s$ ; (2) dry surface condition; (3) daylight condition. The resulting dataset includes  $2.95 \times 10^8$  data points, which are approximately 8,200 driving hours.

The flow chart of data processing is shown in Figure 3. The original data were first segmented into trajectories and then categorized into specific groups based on the driving situations. Then, a smoothing technique was applied to the discretized maneuver distribution and finally, we could obtain the probability mass functions for each group, which constituted the empirical data-driven behavior models. Details of each step are elaborated in the following paragraphs.

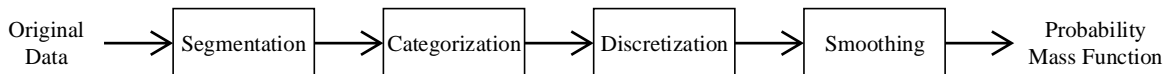


Figure 3: Data processing flow chart.

The original data were first segmented into trajectories with the following requirements: (1) the time should be continuous and does not have discontinuity of more than 2 seconds, (2) the identification of the surrounding vehicles is consistent throughout the trajectory, (3) each trajectory should last more than 3 seconds. Data that are too noisy (with severe speed and/or position oscillations) are discarded. Considering the driving environment of the subject vehicle, trajectory data points will be categorized into the aforementioned groups, correspondingly. An important step in the categorization is to identify the lane-changing event. During this process, around  $1.3 \times 10^5$  lane-changing events are identified by analyzing the lateral distance to the lane markings. Figure

4 shows two examples that the ego-vehicle is doing left and right lane-changing, respectively. Note that the sign of the distance to lane marking differentiates the left and right lane markings. Take Figure 4a as an example, it shows the whole process of a left lane-changing event: the vehicle is approaching the left lane marking and cross the lane when the distance to the left lane marking equals zero, and then change to the maximum (lane width) after entering the target lane. The starting moment and crossing the lane moment of lane-changing events can be identified based on both the distance and slope change of the distance, accordingly. Similar techniques are also utilized for lane-changing detection in a recent study (de Gelder et al., 2020). The starting point of the lane-changing event will be used for generating the lane-changing behavior models.

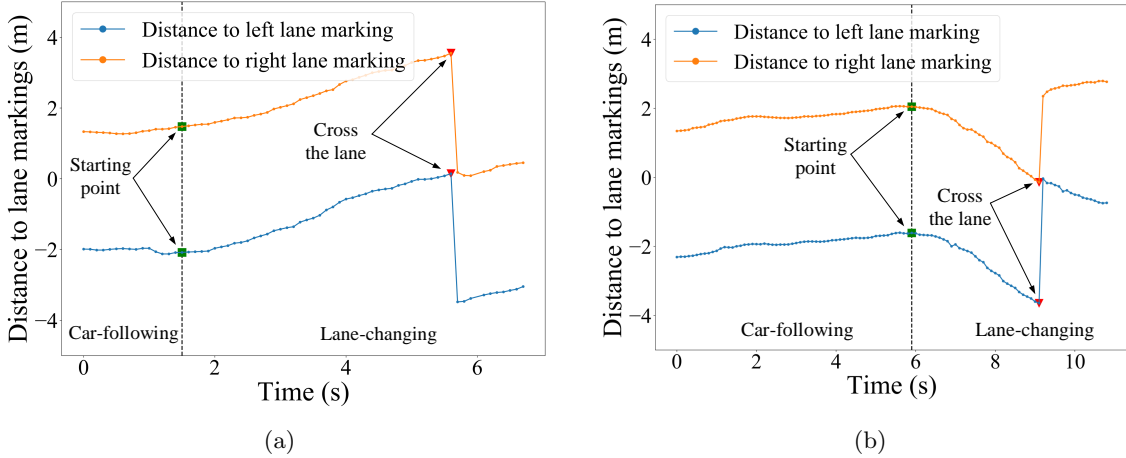


Figure 4: Lane-changing events identification: (a) ego-vehicle is doing a left lane change, (b) ego-vehicle is doing a right lane change.

For each data point, the state was discretized using the following resolutions: except for the speed resolution of longitudinal behavior that is  $0.2\text{ m/s}$ , the speed and spacing resolutions are  $1\text{ m/s}$  and  $1\text{ m}$  for all other situations. The longitudinal acceleration discretization resolution is set as  $0.2\text{ m/s}^2$ . Then, the Moving Average (MA) (Dixon and Massey Jr, 1951) smoothing technique was applied. During the smoothing process, states leading to an inevitable crash will not be included. After that, the empirical probability of each maneuver at each state can be calculated by its frequency in the dataset of the corresponding category. These are the empirical data-driven vehicle behavior models. Figure 5a and Figure 5b show examples of the vehicle longitudinal acceleration distributions given specific states. For both free-driving and car-following cases, the mean of acceleration is around zero, which is consistent with the intuition. And the probability of acceleration greater than zero is generally higher in the free-driving case, which is reasonable as well. Figure 5c to Figure 5f show the lane-changing probability distributions among all states in each category, respectively. We can find that the mean of the lane-changing probability lies around  $10^{-3}$ , which means it takes around 2 minutes on average to perform one discretionary lane-changing maneuver.

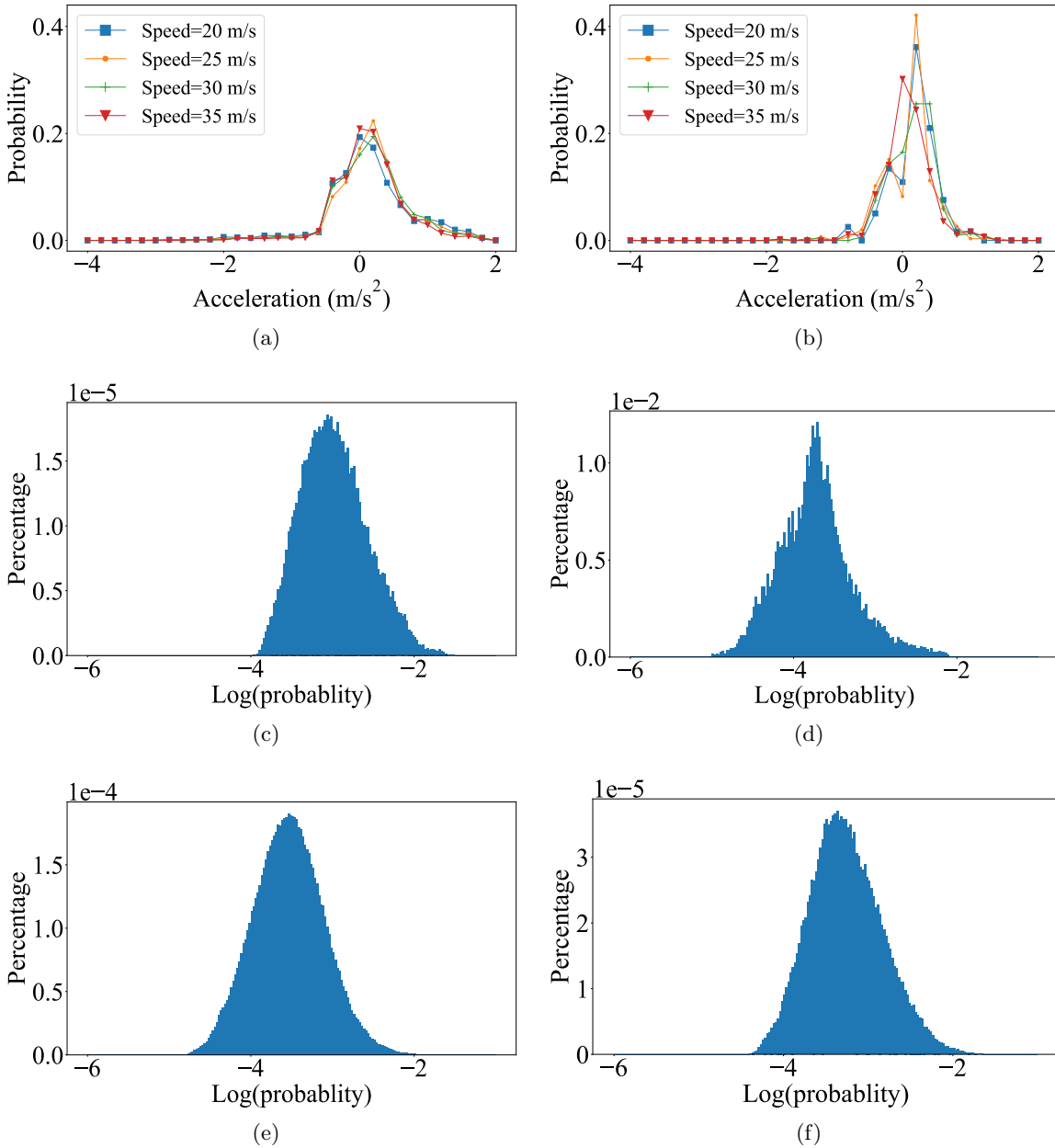


Figure 5: Empirical behavior models demonstration for each category: (a) Free driving, (b) Car following ( $r_1 = 30 m$ ,  $v_1 = v_2$ ), (c) Lane change (Cut in), (d) Lane change (No adjacent vehicle), (e) Lane change (One adjacent vehicle), (f) Lane change (Two adjacent vehicles).

## 4.2 Existing models performance

To demonstrate the performance of existing behavior models and simulation platforms, we conduct simulations using the widely used open-source traffic simulator SUMO (Lopez et al., 2018). Two well-known car-following models, the IDM (Treiber et al., 2000) and the Wiedemann 99 model (VISSIM, 2012) are considered. We use model parameters from multiple sources to fully illustrate the performance. The first category is directly from the literature, which was calibrated by the NDD from Virginia, US (Sangster et al., 2013) (denoted as VT100 IDM), and Shanghai, China (Zhu



et al., 2018a) (denoted as Shanghai IDM and Shanghai W99), respectively. Another category is from the calibration results using the NDD in this study (denoted as SPMD IDM and SPMD W99). The calibration settings and code are based on Hammit et al. (2018) and Hammit (2018). The 80 minutes of car-following data are randomly extracted from different drivers for the calibration process. The SUMO default LC2013 lane-changing model (Erdmann, 2015) was used for the lateral actions. We set the input traffic flow as 1360 vehicles/hour/lane, which belongs to level of service (LOS) C for multilane highways (Federal Highway Administration (FHWA), 1994), and it is the same as the experiments in the following sections for the proposed method. We collected data by simulating these models on a three-lane highway for 35 minutes, respectively, which includes 20 minutes warm-up time and 15 minutes of data collection. One thing to note is that the desired speed of each vehicle in SUMO follows a default Gaussian distribution whose deviation equals 0.1 to incorporate the simulation stochasticity.

To demonstrate the performance, the velocity and range distributions which are important for the AV testing are shown in Figure 6. In general, the velocity and range distributions generated by the simulation are significantly different from the empirical distributions obtained by the NDD. Although the NDD reported in Figure 6a is not the same one used for calibration in the literature, the comparison is still informative: the distribution should naturalistically range among the entire interval, while the simulation results are concentrated in a small interval. Moreover, when models are calibrated using the exact NDD, the resulting distributions still cannot replicate the real-world driving environment as shown in Figure 6b. In addition, we can find from the results that the range is very large since both the IDM and Wiedemann 99 models are designed for accident-free purposes and therefore might be conservative. These NDEs can hardly generate safety-critical scenarios for the AV under test and as a result, may lead to biased evaluation regarding the AV safety performance. These results provide evidence that existing driving behavior models cannot be used directly for the NDE construction for AV testing purposes.

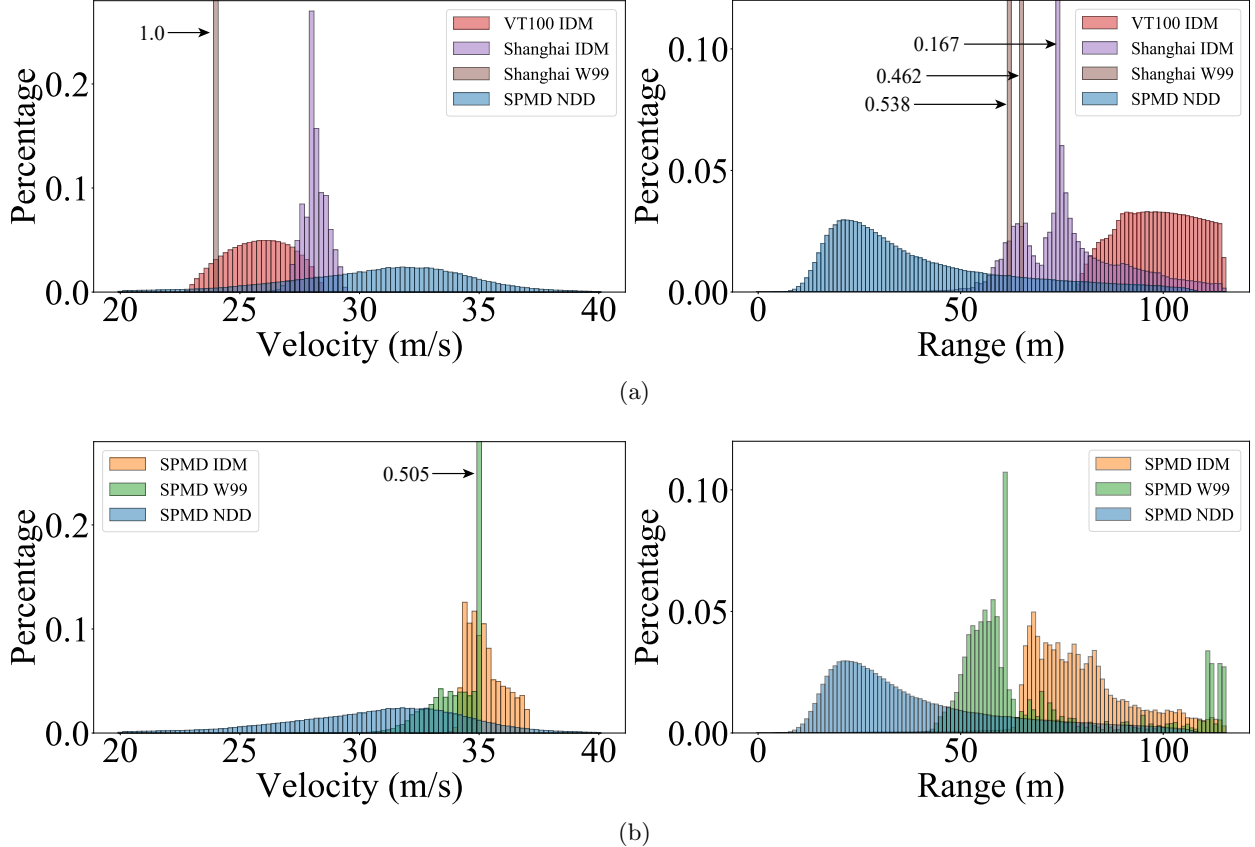


Figure 6: Velocity and range distributions of the NDE using existing methods: (a) model parameters calibrated using NDD from literature, (b) model parameters calibrated using NDD from this study.

### 4.3 Error accumulation problem for empirical behavior models

As the existing driving behavior models cannot reproduce a distributionally consistent NDE, a straightforward method is to directly estimate the behavior models using empirical distributions from NDD, as discussed in Section 2.3. In this section, we demonstrate that the small inaccuracy of empirical behavior models will accumulate and compound along with the simulation.

The simulation platform is developed based on an open-source highway traffic simulator (Leurent, 2018). The bicycle model is implemented to update positions, velocities, and steering angles of all vehicles at a 10Hz frequency. All lane-changing maneuvers are set completed in 1 second. To be consistent with the NDD, the speed of the NDE simulation is bounded between 20 to 40  $m/s$ , and the longitudinal acceleration is bounded between  $-4$  to  $2 m/s^2$ . The size of the initial zone is set as  $d_0 = 50 m$ , and the ratio of car-following cases is  $p_{CF} = 0.68$  according to the NDD. Since both the longitudinal and lateral models are data-driven, it is inevitable there are states where no NDD is collected. We will use the IDM and MOBIL model for states not covered by the proposed behavior models. The SPMD IDM parameters are used, which are calibrated from the NDD. The MOBIL model parameters are partially from Gong et al. (2018) which are also calibrated using the SPMD dataset. The detailed model parameters are listed in the Appendix. B.

We compared the distributions of speed and range between the constructed NDE using empirical behavior models and the ground truth (i.e., empirical distribution from NDD). Two measurements,

the Hellinger distance and the mean absolute error (MAE), are used to quantitatively measure the dissimilarity between the simulated distribution and the true distribution. The smaller the measurement, the similar the two distributions, and the better the model performance. For discrete probability distributions  $P = (p_1, p_2, \dots, p_k)$  and  $Q = (q_1, q_2, \dots, q_k)$  defined on the same probability space, the Hellinger distance between  $P$  and  $Q$  is defined as

$$\text{Hellinger-distance} = \frac{1}{\sqrt{2}} \sqrt{\sum_{i=1}^k (\sqrt{p_i} - \sqrt{q_i})^2}. \quad (39)$$

And the MAE is defined as

$$\text{MAE} = \frac{\sum_{i=1}^k |p_i - q_i|}{k}. \quad (40)$$

We conducted simulations on a three-lane highway. Using the proposed initialization method, around 60 vehicles (equivalents to 1360 vehicles/hour/lane) will be initialized for each simulation. We ran 100 simulations to mitigate the randomness effect, and each simulation ran 15 minutes. The data were collected throughout the simulation. To illustrate the error accumulation process, we would like to evaluate the distributions at both the beginning of the simulation and also after a certain transition period. We show the distributions of speed and range in three time intervals of the simulation as shown in Figure 7. We can find the proposed initialization method performs well, which can generate initial states similar to the NDD. The good initialization states result in good range distribution at the beginning of simulations, however, the velocity distribution starts to deviate from the ground truth as shown in Figure 7a. After 5 minutes transition, the velocity distribution is significantly different from the ground truth as shown in Figure 7b and 7c. Note again that the vehicle velocity in the simulation is bounded by 40  $m/s$ . From these results, we can find that, although starting from a good initialization, the error caused by behavior models will be accumulated, and the resulting environment feature distribution will deviate from the ground truth after a certain period of transition. This is a critical problem for the AV testing application, as AV testing requires a certain period of simulation. Comparing with the range distribution, the velocity distribution suffered more severely from the error accumulation, which is also one reason why we choose the velocity distribution as the optimization target in the robust modeling framework.

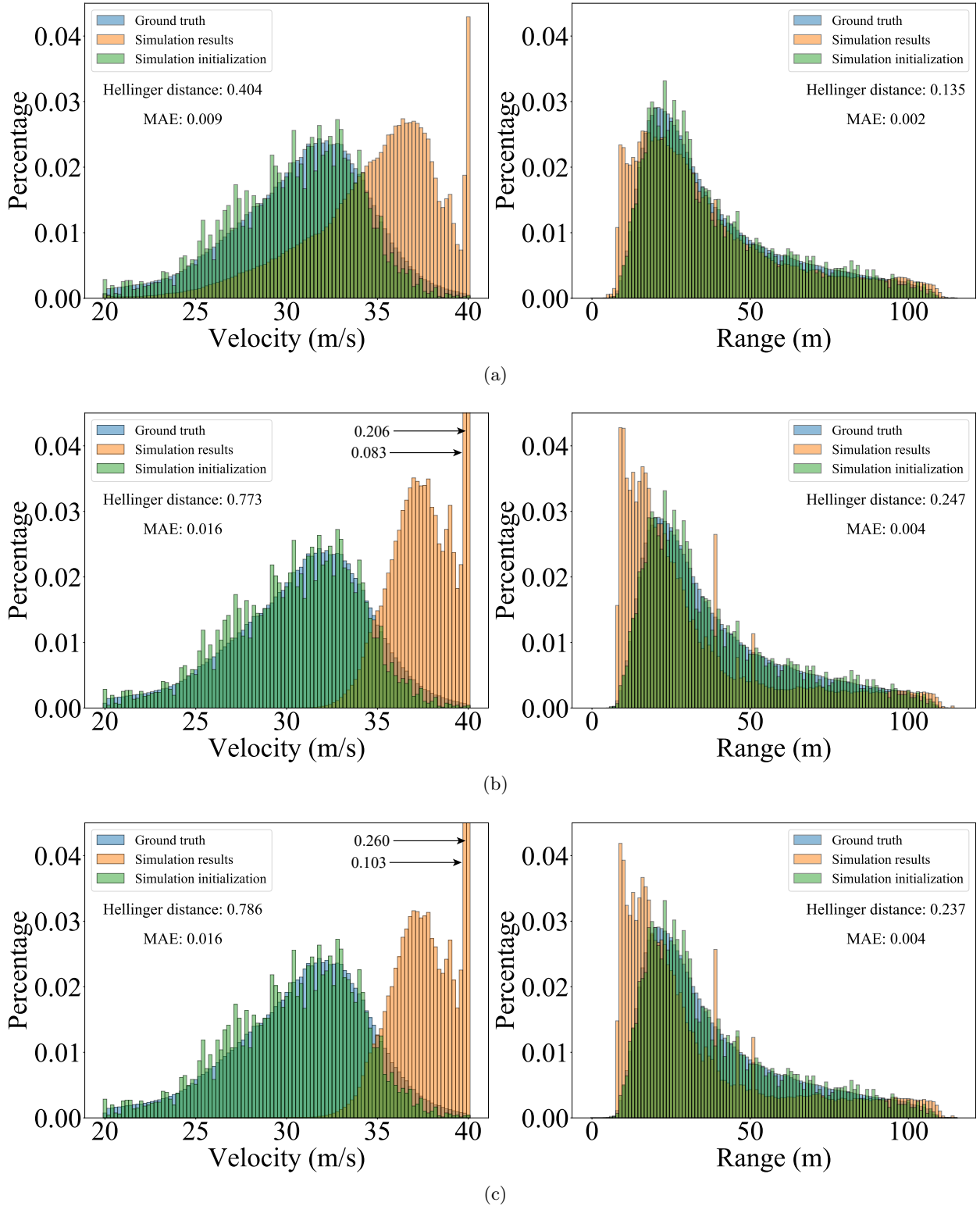


Figure 7: Velocity and range distributions of the NDE using empirical behavior models: (a) first 5 minutes of simulation, (b) mid 5 minutes of simulation, (c) last 5 minutes of simulation.

#### 4.4 Performance of the robust modeling framework

In this section, the performance of the robust modeling framework is examined and demonstrated. Figure 8 shows the simulation results of the proposed NDE after the adjustment of empirical behavior models. The simulation settings are the same as in Section 4.3. The Hellinger distance is around 0.15 and 0.20 for velocity and range distribution, respectively. Comparing with results before the optimization as shown in Figure 7, the velocity distribution is similar to the naturalistic distribution even after a long time transition period, so the error accumulation issue is significantly solved. The range distribution is similar to the one before the optimization, which is close to the ground truth. It indicates that the better performance of the speed distribution does not worsen the spacing distribution. The results show that our method can generate NDE that is distributionally consistent with the real-world driving environment throughout the entire simulation process. Besides, the results also indicate that the proposed NDE does not need a warm-up period since both features match well in the first 5 minutes of the simulation as shown in Figure 8a. This could improve testing efficiency and simplify the testing procedure. Compared with the performance of existing models as shown in Figure 6, the proposed NDE exhibits superior performance, which can better imitate the real-world driving situations for the AV testing purposes.

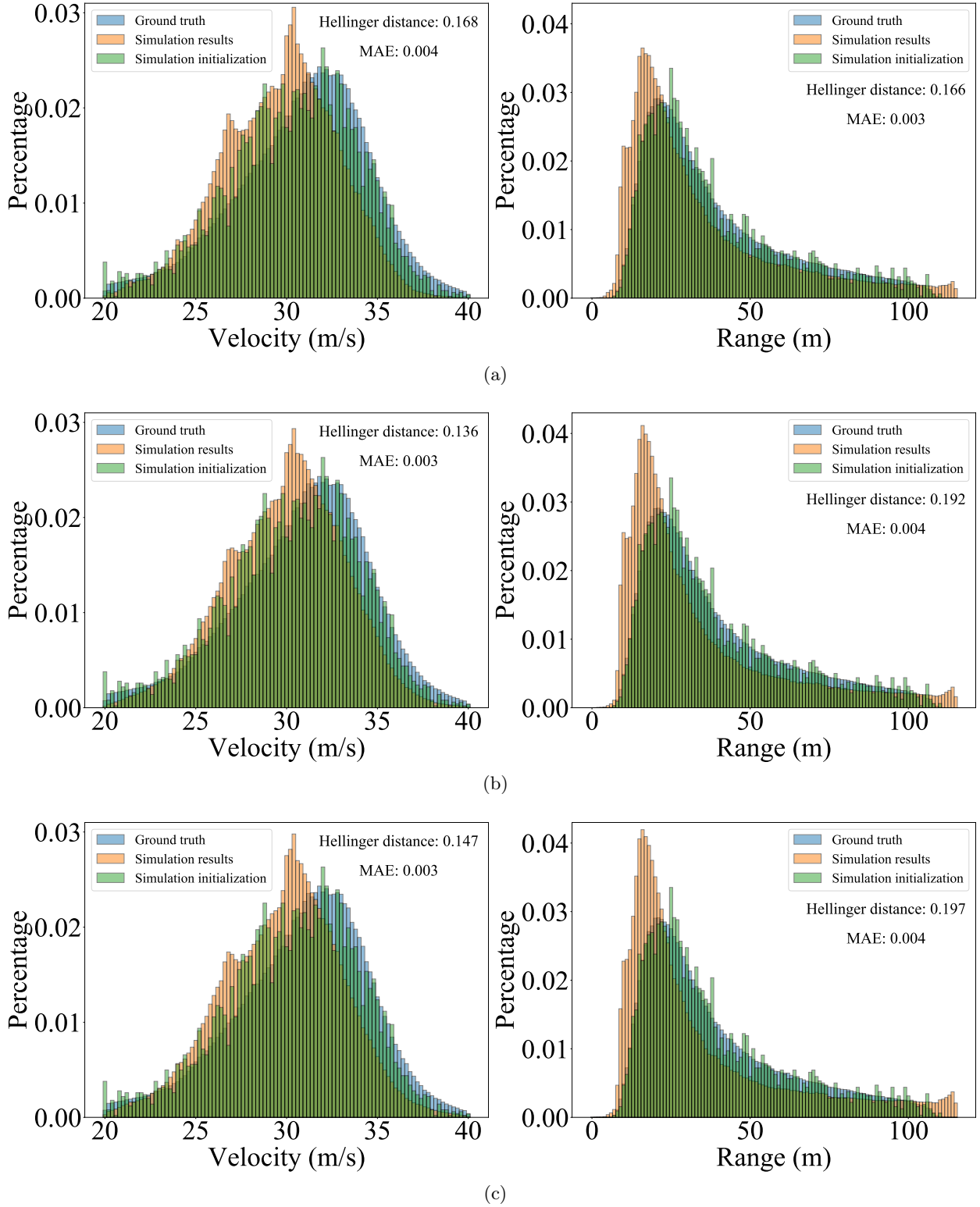


Figure 8: Velocity and range distributions of the proposed NDE using optimized behavior models: (a) first 5 minutes of simulation, (b) mid 5 minutes of simulation, (c) last 5 minutes of simulation.

In addition to the velocity and range distribution, we also calculated the lane-changing statistic

of the proposed NDE to further examine its performance. From the simulation results, the average travel distance for one lane change is 4.86 kilometers. In the real-world driving environment, the same statistic is 4.45 kilometers per lane change on the highway and interstate route (Lee et al., 2004). Therefore, the experiment results show that the proposed NDE can reproduce a reasonable number of lane changes as in the real-world driving environment.

## 4.5 AV testing using the proposed NDE

After validating the proposed NDE performance, we used it to test the AV safety performance to further demonstrate the capability of the proposed NDE on the AV testing application.

### 4.5.1 AV testing settings

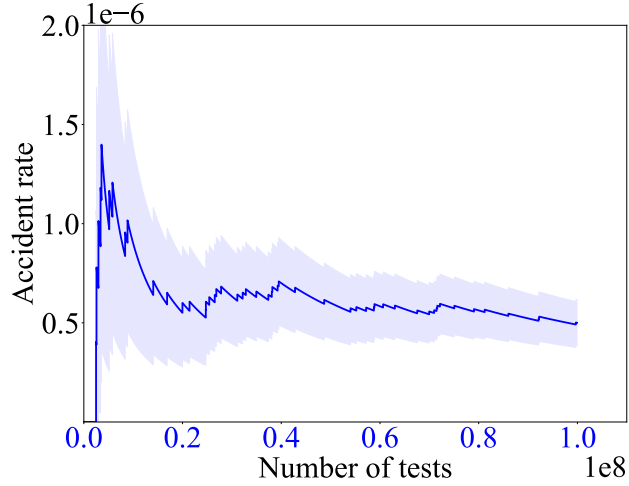
The IDM and MOBIL models are used as the AV model, where the model parameters are listed in the Appendix. C. To measure the AV safety performance, the accident rate of AV in the NDE is chosen as the measurement (Zhao et al., 2016; Feng et al., 2020a,b). Since the NDE is developed to imitate the real-world driving environment, the accident rate evaluated in the NDE can represent the safety performance of the AV in the real world. The Monte Carlo (MC) method was applied to obtain the accident rate. More detailed discussions about the testing measurements can be found in Feng et al. (2020a,b).

For the convenience of experiments, we conducted one simulation test for a constant driving distance (400 *m*) of the AV. The test result, i.e., accident or not, of each simulation is recorded, and then the accident rate per simulation test can be calculated. As the distance of each test is constant, it can easily transform between the accident rate per simulation test and the driving miles.

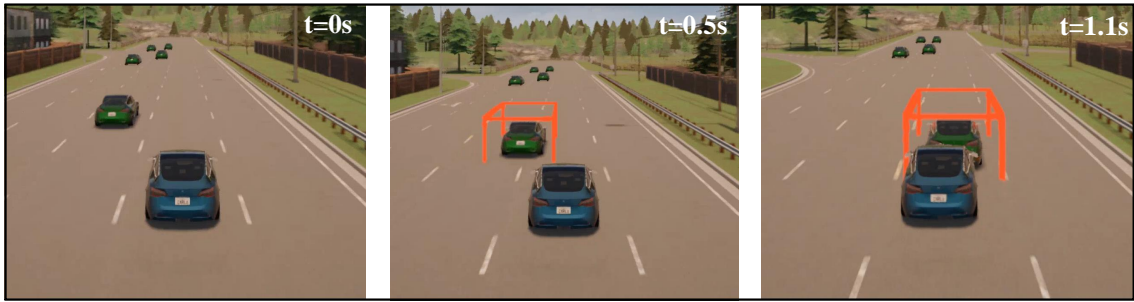
Since the NDE has been shown to well-imitate the real-world driving environment, the accident rate of the AV will be very low and similar to the real-world accident rate. Therefore, more than millions of simulations may be needed to reach an accurate estimation. We conducted the simulations on the University of Michigan’s Great Lakes High-Performance Computing (HPC) cluster using 500 cores (Intel Xeon Gold 6154 processor) and 2500 GB RAM. To accelerate the simulation speed, the simulation resolution is set as 1Hz.

### 4.5.2 AV testing results

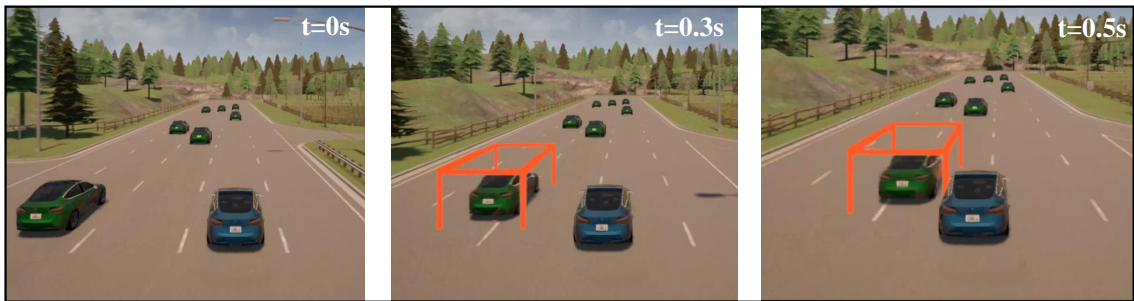
The results of the estimated accident rate are shown in Figure 9a. The shaded area denotes the 90% confidence interval. We ran total  $1 \times 10^8$  simulations and this was approximately 25 million driving miles for the AV under test. The estimated accident rate is  $4.97 \times 10^5$  miles per accident. For human drivers, in the US, the accident rate is  $4.79 \times 10^5$  miles per accident on the highway (Bureau of Transportation Statistics, 2018).



(a)



(b)



(c)

Figure 9: Results of the AV testing and evaluation: (a) estimation results of the accident rate (shaded area denotes the 90% confidence interval), (b) accident case example 1, (c) accident case example 2.

The accident cases are important to analyze the performance of the AV under test and can be further utilized to improve the AV. Especially, for learning-based AV models, the accident cases can serve as adversarial examples which can provide valuable insights for model improvement (Goodfellow et al., 2015). Diverse accident cases can be generated during the test. Two examples of accident cases were selected and rendered using Carla (Dosovitskiy et al., 2017) as shown in



Figure 9b and Figure 9c. The blue vehicle is the AV under test, the green vehicles represent background vehicles, and the green vehicle with the red rectangle represents the principal other vehicle (POV) that crashes with the AV. In the first example, the AV had a rear-end collision with the cut-in POV when the AV was trying to do an evasive lane-changing maneuver. In the second example, the accident happened when the AV under test and the POV were doing the lane change maneuver simultaneously towards the same target lane. This example indicates that adding a behavior prediction module of all surrounding vehicles, including those not on adjacent lanes, might help improve the safety performance of the AV under test. These adversarial examples exhibit the capability of providing insights for the AV model improvements.

## 5 Conclusions

In this paper, we propose a distributionally consistent NDE modeling framework for the AV testing purpose. We first propose to directly generate empirical behavior models using large-scale NDD. These empirical behavior models can serve as basic models, since they will converge in probability to the real behavior models when the data size and quality are sufficiently large and accurate. In order to address the error accumulation problem and guarantee the accuracy of the NDE throughout the simulation, a robust modeling framework based on the Markov process is proposed, which optimizes the empirical models by matching the environment feature distribution with the ground truth. The proposed method is validated for the multilane highway driving environment using large-scale real-world NDD. Two environment features are selected, i.e., speed and spacing, which are important for AV testing. Their distributions generated by the proposed NDE are consistent with real-world empirical distributions. Moreover, the lane-changing statistic is also examined to be consistent with the ground truth, which further validates the proposed NDE. To further illustrate the capability for AV testing, the generated NDE is utilized to test the safety performance of an AV model. The experiment results show that the generated NDE can effectively evaluate AV safety performance and produce diverse accident cases that are valuable for AV improvements.

There are certain limitations in the current work that can be addressed by future research. First, homogenous vehicles are considered in this study where all background vehicles share the same behavior models and vehicle classes. In the real-world driving environment, there are different vehicle classes, such as sedan, truck, and heavy vehicle, etc. Moreover, within a specific vehicle class, they may have different behavior models, for example, some drivers are more aggressive and some drivers are more conservative. Second, the vehicle behavior models in this study are purely data-driven. Incorporating model-based behavior models could potentially benefit the NDE construction process and reduce the data size needed comparing with the purely data-driven methods. We leave these for future research.

## Appendix A

The proof follows Shalizi (2016) is as follows. The empirical behavior models in different traffic state are  $F^* = [f^*(Z^1), \dots, f^*(Z^{|Z|})]$ . We will use a uniform distribution within each discretized state. For a given state  $Z$ , consider the action  $u$  which lies in a bin whose boundaries are  $u_0$  and  $u_0 + b$ , the probability density at  $u$  is estimated using the NDD as

$$f^*(u|Z) = \frac{1}{b} \frac{1}{n} \sum_{i=1}^n \mathbf{1}_{(u_0, u_0+b]}(u_i|Z),$$

where  $n$  is the NDD data size in the given traffic state, and  $\mathbf{1}_{(u_0, u_0+b]}(u_i|Z)$  is the indicator function denotes whether a vehicle chooses the action belongs to the bin given the traffic state. When the NDD is collected following the true behavior distributions, the number of points in the bin will follow a Binomial distribution  $\mathcal{B}(n, p)$ , where  $p$  is the true probability of falling in the bin. The true probability also equals to

$$p = CDF(x_0 + b) - CDF(x_0),$$

where  $CDF(\cdot)$  is the true cumulative density function of the behavior model. Then we have the expectation and variance of the empirical density as

$$\begin{aligned} \mathbb{E}[f^*(u|Z)] &= \frac{1}{nb} \mathbb{E}[\mathcal{B}(n, p)] \\ &= \frac{CDF(x_0 + b) - CDF(x_0)}{b}. \end{aligned}$$

$$\begin{aligned} \text{Var}[f^*(u|Z)] &= \frac{1}{n^2 b^2} \text{Var}[\mathcal{B}(n, p)] \\ &= \mathbb{E}[f^*(u|Z)] \frac{(1 - CDF(x_0 + b) + CDF(x_0))}{nb}. \end{aligned}$$

When the NDD size is infinitely large and the action resolution is infinitely high, i.e.,  $n \rightarrow \infty, b \rightarrow 0$ , then we have

$$\mathbb{E}[f^*(u|Z)] \rightarrow \lim_{b \rightarrow 0} \frac{CDF(x_0 + b) - CDF(x_0)}{b} = f^{\text{true}}(u|Z),$$

since the probability density function is the derivative of the cumulative density function. The  $f^{\text{true}}$  in the equation denotes the true behavior distributions. Therefore, we can find the histogram density estimator is unbiased. Moreover, when  $b \rightarrow 0$  but  $nb \rightarrow \infty$  as  $n \rightarrow \infty$ , the variance will be  $\text{Var}[f^*(u|Z)] \rightarrow 0$ . Therefore, we conclude the proof that the empirical behavior models will converge to the real-world driving behavior models.

## Appendix B

The calibrated parameters of the IDM model using the SPMD are: maximum acceleration ( $0.8 \text{ m/s}^2$ ), desired speed ( $37 \text{ m/s}$ ), exponent parameter (3.0), comfortable deceleration ( $-1.3 \text{ m/s}^2$ ), gap at standstill ( $0.1 \text{ m}$ ), and desired time headway ( $0.8 \text{ s}$ ). To generate a stochastic version IDM, the output acceleration will follows a Gaussian distribution with the original output acceleration as mean and 0.3 as standard deviation. The parameters of the MOBIL model are: politeness factor (0.1), utility threshold ( $0.2 \text{ m/s}^2$ ), and maximum safe deceleration ( $-3 \text{ m/s}^2$ ).

## Appendix C

The parameters for the AV under test are as follows. The parameters of the IDM model are: maximum acceleration ( $1.5 \text{ m/s}^2$ ), desired speed ( $33.33 \text{ m/s}$ ), exponent parameter (4.0), comfortable deceleration ( $-2.0 \text{ m/s}^2$ ), gap at standstill ( $2.0 \text{ m}$ ), and desired time headway ( $1.2 \text{ s}$ ). The parameters of the MOBIL model are: politeness factor (0.0), utility threshold ( $0.1 \text{ m/s}^2$ ), and maximum safe deceleration ( $-4 \text{ m/s}^2$ ).

## Acknowledgments

The authors would like to thank the US Department of Transportation (USDOT) Region 5 University Transportation Center: Center for Connected and Automated Transportation (CCAT) of the University of Michigan for funding the research. The authors would like to thank Dr. Bo Yu for his help in the data querying process. The views presented in this paper are those of the authors alone.

## CRedit author statement

**Xintao Yan:** Conceptualization, Methodology, Software, Data curation, Writing-original draft, Writing-review and editing. **Shuo Feng:** Conceptualization, Methodology, Writing-original draft, Writing-review and editing. **Haowei Sun:** Software. **Henry X. Liu:** Conceptualization, Writing-original draft, Writing-review and editing, Funding acquisition, Supervision.

## References

- Bareiss, D., van den Berg, J., 2015. Generalized reciprocal collision avoidance. *The International Journal of Robotics Research* 34, 1501–1514.
- Bezzina, D., Sayer, J., 2014. Safety pilot model deployment: Test conductor team report. Report No. DOT HS 812, 18.
- Bhattacharyya, R., Wulfe, B., Phillips, D., Kuefler, A., Morton, J., Senanayake, R., Kochenderfer, M., 2020. Modeling human driving behavior through generative adversarial imitation learning. [arXiv:2006.06412](https://arxiv.org/abs/2006.06412).
- Bureau of Transportation Statistics, 2018. Transportation accidents by mode. <https://www.bts.gov/content/transportation-accidents-mode>. [Online].
- Chen, X., Li, L., Zhang, Y., 2010. A markov model for headway/spacing distribution of road traffic. *IEEE Transactions on Intelligent Transportation Systems* 11, 773–785.
- Dixon, W.J., Massey Jr, F.J., 1951. *Introduction to statistical analysis*. McGraw-Hill.
- Dosovitskiy, A., Ros, G., Codevilla, F., Lopez, A., Koltun, V., 2017. Carla: An open urban driving simulator. [arXiv:1711.03938](https://arxiv.org/abs/1711.03938).
- Erdmann, J., 2015. Sumo lane-changing model, in: *Modeling Mobility with Open Data*. Springer, pp. 105–123.
- Federal Highway Administration (FHWA), 1994. *Highway Capacity Manual, Special Report 209*. Transportation Research Board, National Research Council.
- Feng, S., Feng, Yiheng and Yu, C., Zhang, Y., Liu, H.X., 2020a. Testing scenario library generation for connected and automated vehicles, part I: Methodology. *IEEE Transactions on Intelligent Transportation Systems* doi:[10.1109/TITS.2020.2972211](https://doi.org/10.1109/TITS.2020.2972211).
- Feng, S., Feng, Yiheng and Sun, H., Bao, S., Zhang, Y., Liu, H.X., 2020b. Testing scenario library generation for connected and automated vehicles, part II: Case studies. *IEEE Transactions on Intelligent Transportation Systems* doi:[10.1109/TITS.2020.2988309](https://doi.org/10.1109/TITS.2020.2988309).
- Feng, S., Feng, Yiheng and Sun, H., Zhang, Y., Liu, H.X., 2020c. Testing scenario library generation for connected and automated vehicles: An adaptive framework. *IEEE Transactions on Intelligent Transportation Systems* doi:[10.1109/TITS.2020.3023668](https://doi.org/10.1109/TITS.2020.3023668).
- Feng, S., Feng, Yiheng and Yan, X., Shen, S., Xu, S., Liu, H.X., 2020d. Safety assessment of highly automated driving systems in test tracks: a new framework. *Accident Analysis & Prevention* 144, 105664.
- de Gelder, E., Manders, J., Grappiolo, C., Paardekooper, J.P., den Camp, O.O., Schutter, B.D., 2020. Real-world scenario mining for the assessment of automated vehicles. [arXiv:2006.00483](https://arxiv.org/abs/2006.00483).
- Gipps, P.G., 1981. A behavioural car-following model for computer simulation. *Transportation Research Part B: Methodological* 15, 105–111.
- Gipps, P.G., 1986. A model for the structure of lane-changing decisions. *Transportation Research Part B: Methodological* 20, 403–414.

- Gong, X., Guo, Y., Feng, Y., Sun, J., Zhao, D., 2018. Evaluation of the energy efficiency in a mixed traffic with automated vehicles and human controlled vehicles, in: 2018 21st International Conference on Intelligent Transportation Systems (ITSC), IEEE. pp. 1981–1986.
- Goodfellow, I.J., Shlens, J., Szegedy, C., 2015. Explaining and harnessing adversarial examples. [arXiv:1412.6572](https://arxiv.org/abs/1412.6572).
- Grimmett, G., Stirzaker, D., 2020. Probability and random processes. Oxford university press.
- Hamdar, S.H., Mahmassani, H.S., Treiber, M., 2015. From behavioral psychology to acceleration modeling: Calibration, validation, and exploration of drivers’ cognitive and safety parameters in a risk-taking environment. *Transportation Research Part B: Methodological* 78, 32–53.
- Hamdar, S.H., Treiber, M., Mahmassani, H.S., Kesting, A., 2008. Modeling driver behavior as sequential risk-taking task. *Transportation research record* 2088, 208–217.
- Hammit, B., 2018. A case for online traffic simulation: Systematic procedure to calibrate car-following models using vehicle data. <https://github.com/bhammit1/Analysis>.
- Hammit, B., James, R., Ahmed, M., 2018. A case for online traffic simulation: Systematic procedure to calibrate car-following models using vehicle data, in: 2018 21st International Conference on Intelligent Transportation Systems (ITSC), IEEE. pp. 3785–3790.
- He, Z., Zheng, L., Guan, W., 2015. A simple nonparametric car-following model driven by field data. *Transportation Research Part B: Methodological* 80, 185–201.
- Huang, X., Sun, J., Sun, J., 2018. A car-following model considering asymmetric driving behavior based on long short-term memory neural networks. *Transportation research part C: emerging technologies* 95, 346–362.
- Hungar, H., Köster, F., Mazzega, J., 2017. Test specifications for highly automated driving functions: Highway pilot.
- Jabari, S.E., Zheng, J., Liu, H.X., 2014. A probabilistic stationary speed–density relation based on newell’s simplified car-following model. *Transportation Research Part B: Methodological* 68, 205–223.
- Kalra, N., Paddock, S.M., 2016. Driving to safety: How many miles of driving would it take to demonstrate autonomous vehicle reliability? *Transportation Research Part A: Policy and Practice* 94, 182–193.
- Kesting, A., Treiber, M., Helbing, D., 2007. General lane-changing model MOBIL for car-following models. *Transportation Research Record* 1999, 86–94.
- Klischat, M., Althoff, M., 2020. Synthesizing traffic scenarios from formal specifications for testing automated vehicles, in: *Proc. of the IEEE Intelligent Vehicles Symposium*.
- Koren, M., Alsaif, S., Lee, R., Kochenderfer, M.J., 2018. Adaptive stress testing for autonomous vehicles, in: 2018 IEEE Intelligent Vehicles Symposium (IV), IEEE. pp. 1–7.
- Kuefler, A., Morton, J., Wheeler, T., Kochenderfer, M., 2017. Imitating driver behavior with generative adversarial networks, in: 2017 IEEE Intelligent Vehicles Symposium (IV), IEEE. pp. 204–211.

- Laval, J.A., Toth, C.S., Zhou, Y., 2014. A parsimonious model for the formation of oscillations in car-following models. *Transportation Research Part B: Methodological* 70, 228–238.
- Lee, S.E., Olsen, E.C., Wierwille, W.W., et al., 2004. A comprehensive examination of naturalistic lane-changes. Technical Report. United States. Department of Transportation. National Highway Traffic Safety Administration.
- Leurent, E., 2018. An environment for autonomous driving decision-making. <https://github.com/eleurent/highway-env>.
- Li, L., Chen, X.M., 2017. Vehicle headway modeling and its inferences in macroscopic/microscopic traffic flow theory: A survey. *Transportation Research Part C: Emerging Technologies* 76, 170–188.
- Li, L., Chen, X.M., Zhang, L., 2016. A global optimization algorithm for trajectory data based car-following model calibration. *Transportation Research Part C: Emerging Technologies* 68, 311–332.
- Li, L., Wang, X., Wang, K., Lin, Y., Xin, J., Chen, L., Xu, L., Tian, B., Ai, Y., Wang, J., Cao, D., Liu, Y., Wang, C., Zheng, N., Wang, F.Y., 2019a. Parallel testing of vehicle intelligence via virtual-real interaction. *Science Robotics* doi:[10.1126/scirobotics.aaw4106](https://doi.org/10.1126/scirobotics.aaw4106).
- Li, W., Pan, C., Zhang, R., Ren, J., Ma, Y., Fang, J., Yan, F., Geng, Q., Huang, X., Gong, H., et al., 2019b. AADS: Augmented autonomous driving simulation using data-driven algorithms. *Science Robotics* doi:[10.1126/scirobotics.aaw0863](https://doi.org/10.1126/scirobotics.aaw0863).
- Lopez, P.A., Behrisch, M., Bieker-Walz, L., Erdmann, J., Flötteröd, Y.P., Hilbrich, R., Lücken, L., Rummel, J., Wagner, P., WieBner, E., 2018. Microscopic traffic simulation using SUMO, in: 2018 21st International Conference on Intelligent Transportation Systems (ITSC), IEEE. pp. 2575–2582.
- Newell, G.F., 1965. Instability in dense highway traffic: a review.
- Newell, G.F., 2002. A simplified car-following theory: a lower order model. *Transportation Research Part B: Methodological* 36, 195–205.
- O’Kelly, M., Sinha, A., Namkoong, H., Tedrake, R., Duchi, J.C., 2018. Scalable end-to-end autonomous vehicle testing via rare-event simulation. *Advances in Neural Information Processing Systems* 31, 9827–9838.
- Osorio, C., Punzo, V., 2019. Efficient calibration of microscopic car-following models for large-scale stochastic network simulators. *Transportation Research Part B: Methodological* 119, 156–173.
- Owen, A.B., 2013. Monte Carlo theory, methods and examples.
- Punzo, V., Ciuffo, B., Montanino, M., 2012. Can results of car-following model calibration based on trajectory data be trusted? *Transportation research record* 2315, 11–24.
- Sangster, J., Rakha, H., Du, J., 2013. Application of naturalistic driving data to modeling of driver car-following behavior. *Transportation research record* 2390, 20–33.

- Sayer, J., LeBlanc, D., Bogard, S., Funkhouser, D., Bao, S., Buonarosa, M.L., Blankespoor, A., et al., 2011. Integrated Vehicle-Based Safety Systems Field Operational Test: Final Program Report. Technical Report. United States. Joint Program Office for Intelligent Transportation Systems.
- Shalizi, C., 2016. Advanced data analysis from an elementary point of view. Cambridge University Press.
- Thorn, E., Kimmel, S.C., Chaka, M., Hamilton, B.A., et al., 2018. A framework for automated driving system testable cases and scenarios. Technical Report. United States. Department of Transportation. National Highway Traffic Safety Administration.
- Treiber, M., Hennecke, A., Helbing, D., 2000. Congested traffic states in empirical observations and microscopic simulations. *Physical review E* 62, 1805.
- Treiber, M., Kesting, A., 2017. The intelligent driver model with stochasticity-new insights into traffic flow oscillations. *Transportation research procedia* 23, 174–187.
- United States. Department of Transportation, 2020. Ensuring American Leadership in Automated Vehicle Technologies: Automated Vehicles 4.0. <https://www.transportation.gov/sites/dot.gov/files/2020-02/EnsuringAmericanLeadershipAVTech4.pdf>.
- VISSIM, 2012. Vissim 5.40-01, User Manual. Planung Transport Verkehr AG, Karlsruhe, Germany.
- Wang, X., Jiang, R., Li, L., Lin, Y., Zheng, X., Wang, F.Y., 2017. Capturing car-following behaviors by deep learning. *IEEE Transactions on Intelligent Transportation Systems* 19, 910–920.
- Waymo, L., 2020. Waymo safety report. <https://storage.googleapis.com/sdc-prod/v1/safety-report/2020-09-waymo-safety-report.pdf>.
- Wiedemann, R., 1974. Simulation des strassenverkehrsflusses. In: Proceedings of the Schriftenreihe des instituts fir Verkehrswesen der Universitiit Karlsruhe, Germany.
- Xie, D.F., Fang, Z.Z., Jia, B., He, Z., 2019. A data-driven lane-changing model based on deep learning. *Transportation research part C: emerging technologies* 106, 41–60.
- Yang, H.H., Peng, H., 2010. Development of an errorable car-following driver model. *Vehicle System Dynamics* 48, 751–773.
- Yeo, H., 2008. Asymmetric microscopic driving behavior theory. Ph.D. thesis. University of California, Berkeley.
- Zhang, X., Sun, J., Qi, X., Sun, J., 2019. Simultaneous modeling of car-following and lane-changing behaviors using deep learning. *Transportation research part C: emerging technologies* 104, 287–304.
- Zhao, D., Lam, H., Peng, H., Bao, S., LeBlanc, D.J., Nobukawa, K., Pan, C.S., 2016. Accelerated evaluation of automated vehicles safety in lane-change scenarios based on importance sampling techniques. *IEEE transactions on intelligent transportation systems* 18, 595–607.
- Zhu, M., Wang, X., Tarko, A., et al., 2018a. Modeling car-following behavior on urban expressways in shanghai: A naturalistic driving study. *Transportation research part C: emerging technologies* 93, 425–445.

Zhu, M., Wang, X., Wang, Y., 2018b. Human-like autonomous car-following model with deep reinforcement learning. *Transportation research part C: emerging technologies* 97, 348–368.